SOI: 1.1/TAS DOI: 10.15863/TAS
International Scientific Journal
Theoretical & Applied Science

p-ISSN: 2308-4944 (print) **e-ISSN:** 2409-0085 (online)

Year: 2020 **Issue:** 11 **Volume:** 91

Published: 28.11.2020 **http://T-Science.org**

QR – Issue QR – Article

Denis Chemezov
Vladimir Industrial College
M.Sc.Eng., Corresponding Member of International Academy of Theoretical and Applied Sciences, Lecturer, Russian Federation
https://orcid.org/0000-0002-2747-552X
vic-science@yandex.ru

Aleksandr Petrenko
Vladimir Industrial College
Master of Industrial Training, Russian Federation

Aleksey Averyanov
Vladimir Industrial College
Student, Russian Federation

Elena Stepanova
Vladimir Industrial College
Lecturer, Russian Federation

Marina Sergeeva
Vladimir Industrial College
Honorary Worker of Primary Professional Education of the Russian Federation, Master of Industrial Training, Russian Federation

Dmitriy Satarin
Vladimir Industrial College
Student, Russian Federation

2D AND 3D PROFILES OF FLAT SURFACES AFTER HIGH-SPEED MILLING

***Abstract**: The profiles of the flat surfaces after milling the billet made of aluminum alloy are presented in the article. The most optimal cutting mode, taking into account the high milling performance and low roughness of the machined surface, was determined by varying the rotational speed of the end milling cutter, the cutting depth and the feed rate of the billet. The machining modes were taken based on the technical characteristics of the DMC 635 V ecoline (DMG MORI) high-precision numerically controlled milling machine.*

***Key words**: the billet, the end milling cutter, the surface roughness, the machining mode, the experiment.*
***Language**: English*
***Citation**: Chemezov, D., et al. (2020). 2D and 3D profiles of flat surfaces after high-speed milling. *ISJ Theoretical & Applied Science, 11 (91),* 475-484.
***Soi**: http://s-o-i.org/1.1/TAS-11-91-76 ***Doi**: crossref https://dx.doi.org/10.15863/TAS.2020.11.91.76
***Scopus ASCC**: 2209.*

Introduction

The surface quality affects the operational properties of the machines parts. The machined surface of any geometric shape is characterized by the values of roughness, waviness, hardness, residual stresses, and deformation of the crystal lattice of material. The surface roughness is an aggregate of irregularities with the relatively small steps on the reference length [1]. The low surfaces roughness ensures reliable coupling of two or more machines parts and high accuracy of measurements. Machining the billet surface must be performed at the high cutting speeds and the low feed rates for achieving low roughness. The cutting depth should be minimal for elimination of heat in the cutting zone. However, the machining performance is reduced in the conditions of the mass production.

Machining is the most commonly used method for manufacturing the machines parts. Milling is removing allowance from the billet by means of the various milling cutters. The roughness formation of the machined surface of the part when milling on the machine with the computer numerical control (CNC) is presented in the number of the scientific works [2-9]. Since milling takes place in the conditions of removing variable allowance and constantly cutting the teeth into the billet material, it is necessary to increase rigidity of the cutting tool and the billet for reducing the surface roughness.

The optimal milling modes for the certain range of the cutting tool rotational speeds, the cutting depths, and the billet feed rates can be determined after the complex data processing of the multi-factor experiment, which includes the analysis of the high-quality three-dimensional images of roughness and waviness of the surface.

Materials and methods

The experiment consisted in machining the billet with the milling cutters and subsequent studying the surface roughness on the microscope. The plate made of aluminum alloy was used as the billet, since the experiment was performed at the high milling speeds. The billet was pre-machined on the universal milling machine for ensuring the necessary dimensions, the geometric shapes and the surfaces arrangement. The billet dimensions are presented in the Fig. 1.

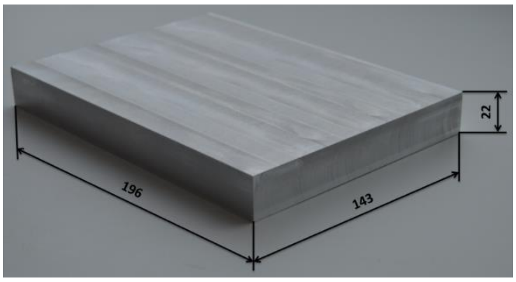

Figure 1 – The billet dimensions.

The open grooves were machined by the high-speed and carbide end milling cutters with the diameter of 10 mm on the wide flat surfaces of the billet. Three cutting teeth were used for the high-speed milling cutter, and two cutting teeth were used for the carbide milling cutter. The tools for milling the open grooves on the billet are presented in the Fig. 2. Machining was carried out on the DMC 635 V ecoline CNC milling machine. This machine allows to perform high-speed machining of the parts made of steels and non-ferrous alloys. The DMC 635 V ecoline CNC machine has the following technical characteristics: moving along the *X*-axis – 635 mm; moving along the *Y*-axis – 510 mm; moving along the *Z*-axis – 460 mm; the maximum spindle rotational speed – 12000 rpm; the drive power – 13 kW; the torque – 83 N×m; the feed force – 5 kN; the feed rate – 24 m/min; positioning accuracy – ISO 230-2; the tools number – 30; the maximum tools weight – 6 kg; the maximum tool length – 300 mm; the maximum tool diameter – 80 mm; the table load – 600 kg; the power consumption at 100% power-on duration – 17 kVA; the control system – 15" DMG MORI SLIMline® with Operate on SIEMENS. The technological equipment for performing the experiment is presented in the Fig. 3.

Figure 2 – The tools for milling: the high-speed end milling cutter with the diameter of 10 mm (left); the carbide end milling cutter with the diameter of 10 mm (right).

A *B*

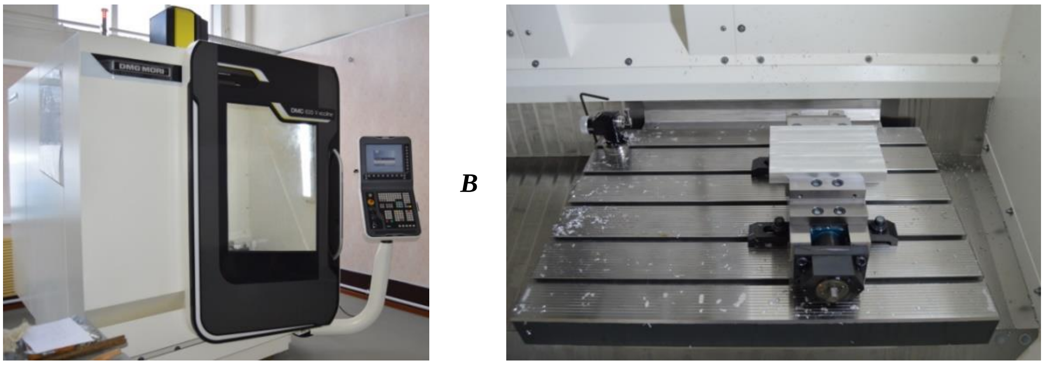

Figure 3 – The general view of the DMC 635 V ecoline CNC milling machine (*A*) and the installation scheme of the billet on the machine table for performing the experiment (*B*).

Machining was carried out using the ECOCOOL 68 CF3 universal water-miscible coolant. The coolant was supplied to the cutting zone under pressure of 3.7 bar.

The experiment was implemented on the various milling modes. The minimum and maximum values of each mode were accepted: the rotational speed of the cutting tool *n* – 2000 and 10000 rpm; the cutting depth *t* – 0.25 and 1.5 mm; the billet feed *S* – 300 and 1500 m/min. Since the number of the accepted factors was three and the levels number was two, it was necessary to perform eight tests in accordance with the planning matrix [10] for conducting the complete multi-factor experiment. The planning matrix of the multi-factor experiment is presented in the table 1.

Table 1. The planning matrix of the experiment.

Test number	*n*, rpm	*t*, mm	*S*, m/min
1	2000	0.25	300
2	10000	0.25	300
3	2000	1.5	300
4	10000	1.5	300
5	2000	0.25	1500
6	10000	0.25	1500
7	2000	1.5	1500
8	10000	1.5	1500

The laboratory studies of the profile of the machined surfaces of the billet were performed using the 4XB metallographic microscope. The equipment is equipped with the digital video camera for taking microphotographs. The microscope has the following technical characteristics: the magnification – 100x-1250x; the length of the mechanical tube – 160 mm; the adjustment range (the microfocus) – 7 mm; the discreteness (the microfocus) – 0.002 mm; the rough adjustment range – 7 mm; the mechanical table – 75×50 mm; the illuminating lamp – 6 V, 12 W (the bromine-tungsten lamp). The general view of the 4XB digital metallographic microscope is presented in the Fig. 4.

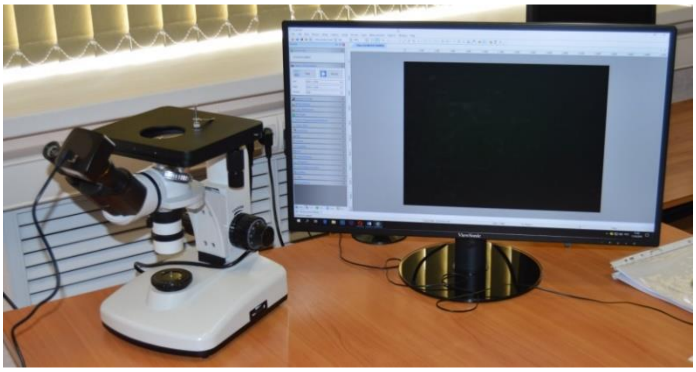

Figure 4 – The 4XB metallographic microscope, connected to the computer, for studying roughness of the machined surfaces of the billet.

Results and discussion

The machined surfaces of the billet on the various milling modes are presented in the Fig. 5. The images show the visual presentation of the quality of the machined billet surfaces. The numbers on the billet are the numbers of the tests performed in accordance with the planning matrix of the multi-factor experiment. The more detailed image of the macrostructure of the machined surfaces of the billet was obtained at the 100x magnification on the microscope.

A

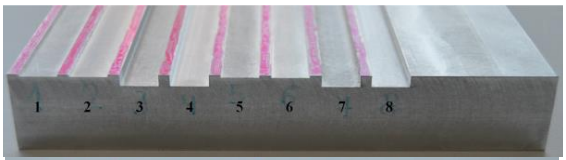

B

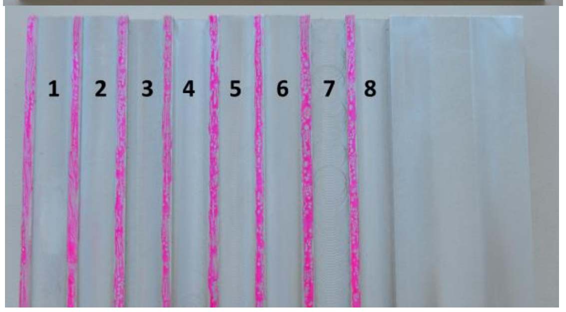

Figure 5 – The machined surfaces of the billet: *A* – the side view; *B* – the top view.

Roughness of the machined surfaces of the billet was measured at the reference length of 15 mm in the longitudinal direction. The step (through which the surface image was captured) was accepted 1 mm. 15 images of the machined surfaces of the billet were stitched into one panoramic image. The panoramic image of the machined surface was presented in the 2D and 3D formats. The 2D and 3D images of the machined surfaces of the billet on the different milling modes are presented in the Figs. 6-21.

Increasing the machining performance by increasing the billet feed must be implemented in compliance with the necessary requirements for the quality of the machined surface. The best result is provided when high-speed semi-finishing machining with the high-speed milling cutter (the eighth milling mode). High-speed machining with the carbide milling cutter leads to a decrease in the surface quality. However, reducing the billet feed at the high rotational speed of the tool and removing the maximum accepted layer of material from the billet allow to get low roughness of the machined surface (the fourth milling mode). The waviness value of the machined surface depends on the feed rate of the billet. The waviness value is shown by the boundaries of the color scheme on the machined surfaces. The most complete profile of the flat surface is observed after machining with the carbide milling cutter on the first and fourth modes.

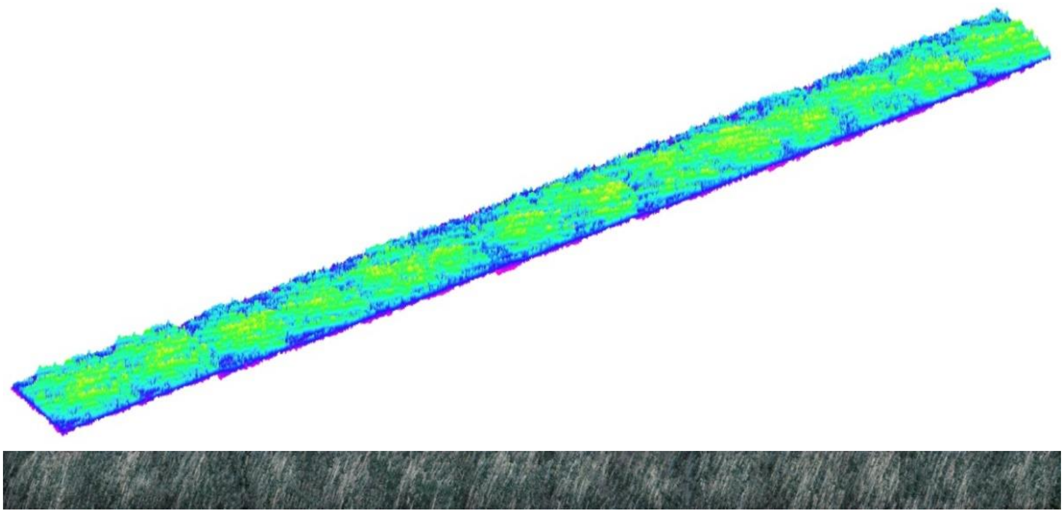

Figure 6 – The 2D and 3D images of the surfaces machined with the high-speed milling cutter (the first mode).

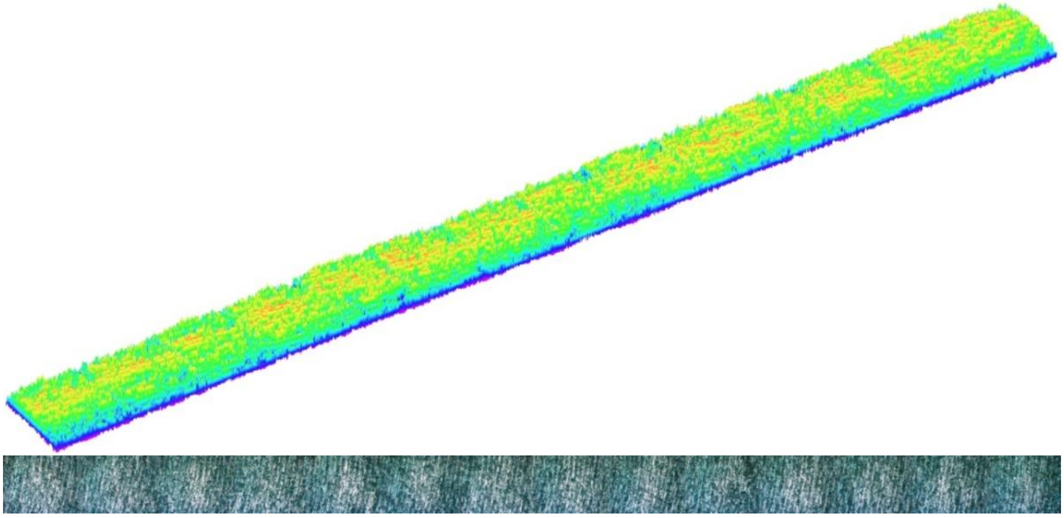

Figure 7 – The 2D and 3D images of the surfaces machined with the carbide milling cutter (the first mode).

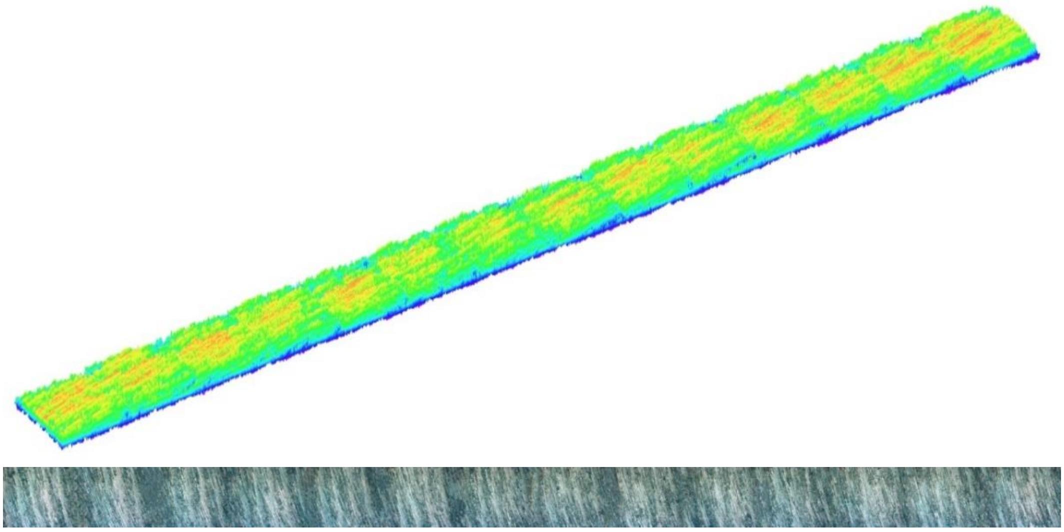

Figure 8 – The 2D and 3D images of the surfaces machined with the high-speed milling cutter (the second mode).

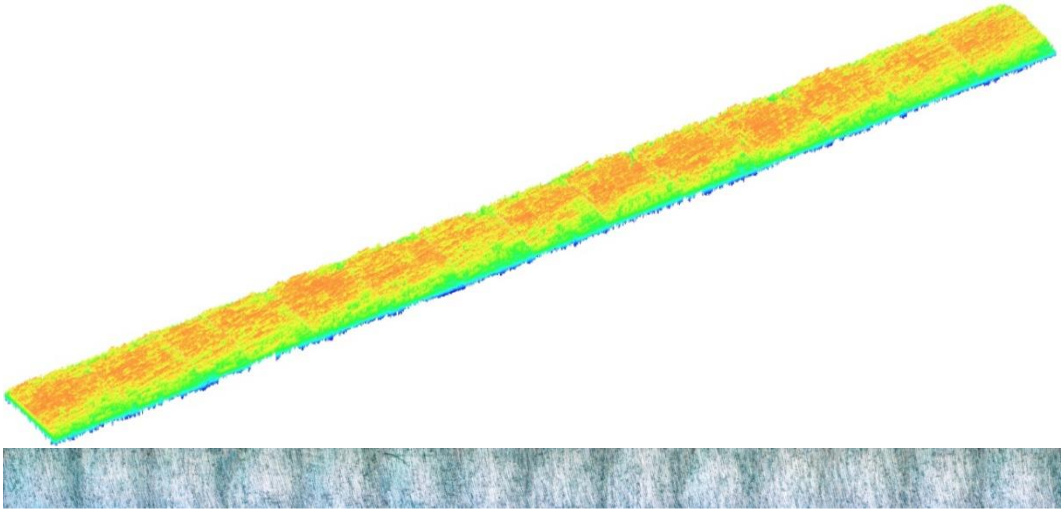

Figure 9 – The 2D and 3D images of the surfaces machined with the carbide milling cutter (the second mode).

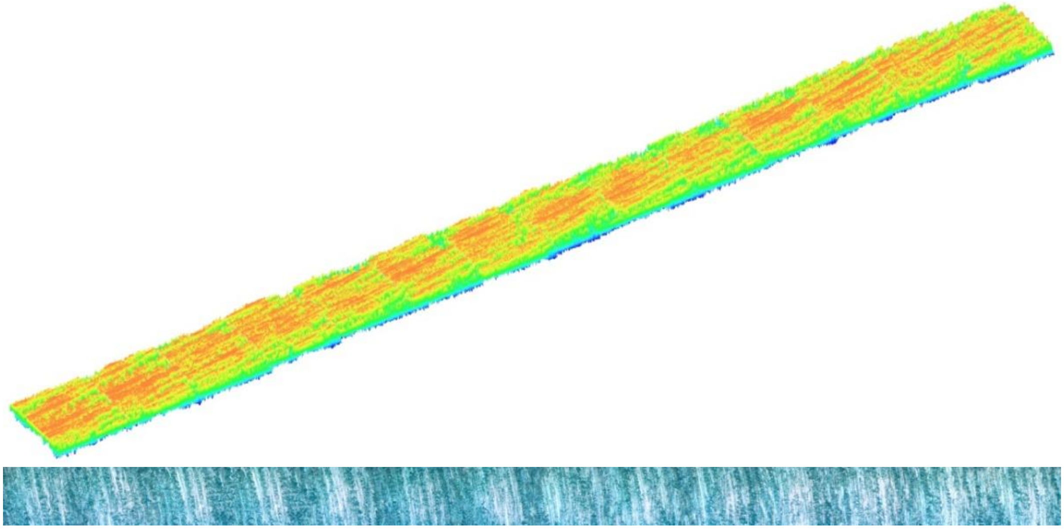

Figure 10 – The 2D and 3D images of the surfaces machined with the high-speed milling cutter (the third mode).

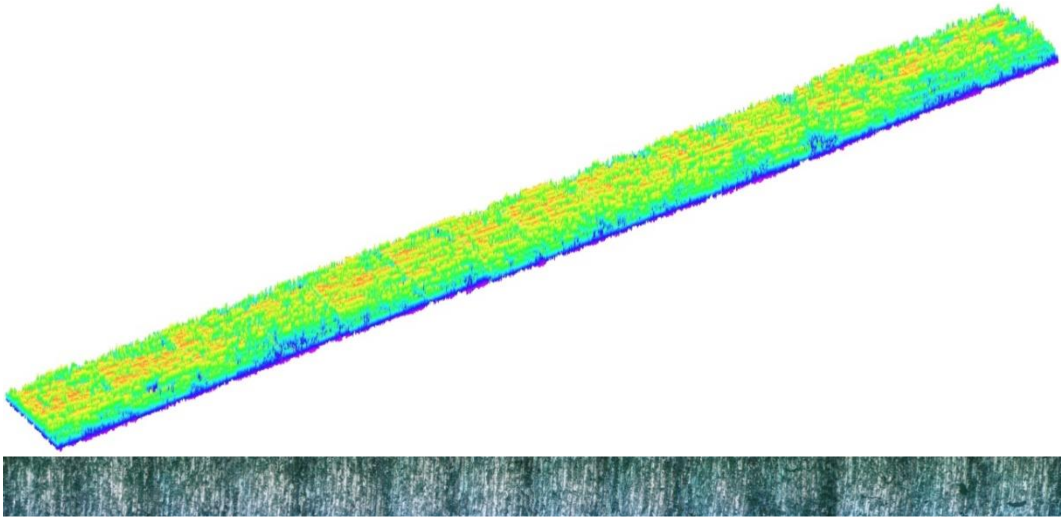

Figure 11 – The 2D and 3D images of the surfaces machined with the carbide milling cutter (the third mode).

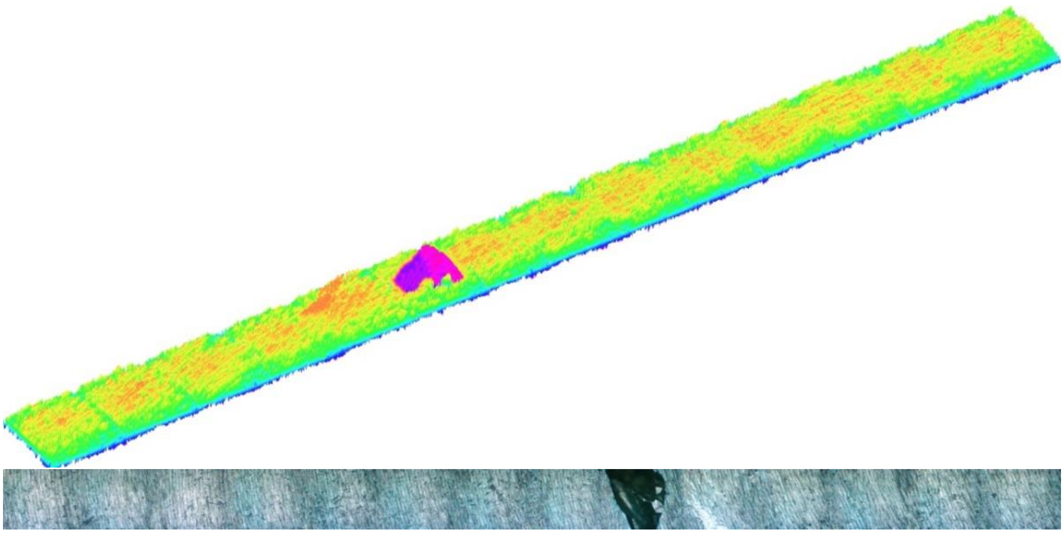

Figure 12 – The 2D and 3D images of the surfaces machined with the high-speed milling cutter (the fourth mode).

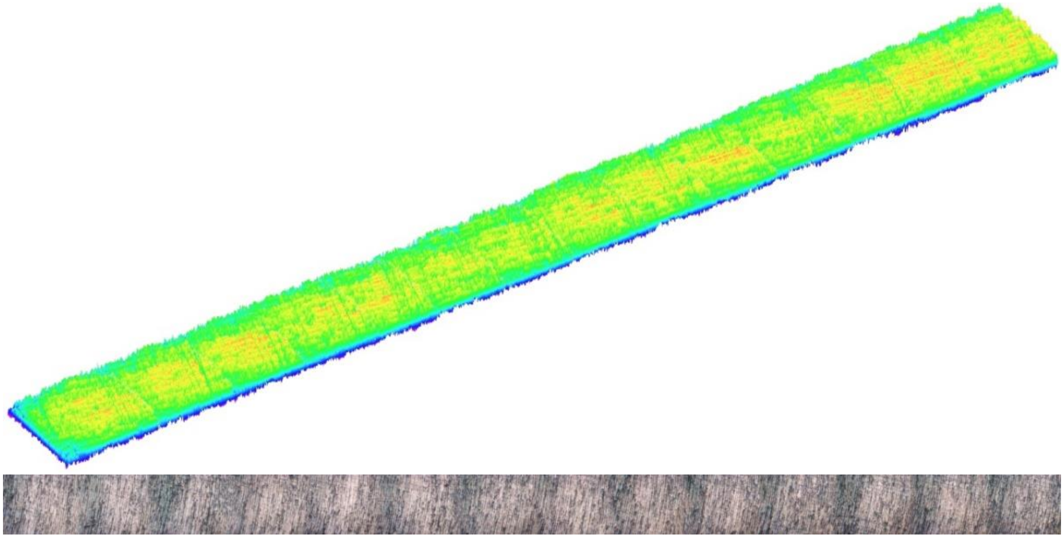

Figure 13 – The 2D and 3D images of the surfaces machined with the carbide milling cutter (the fourth mode).

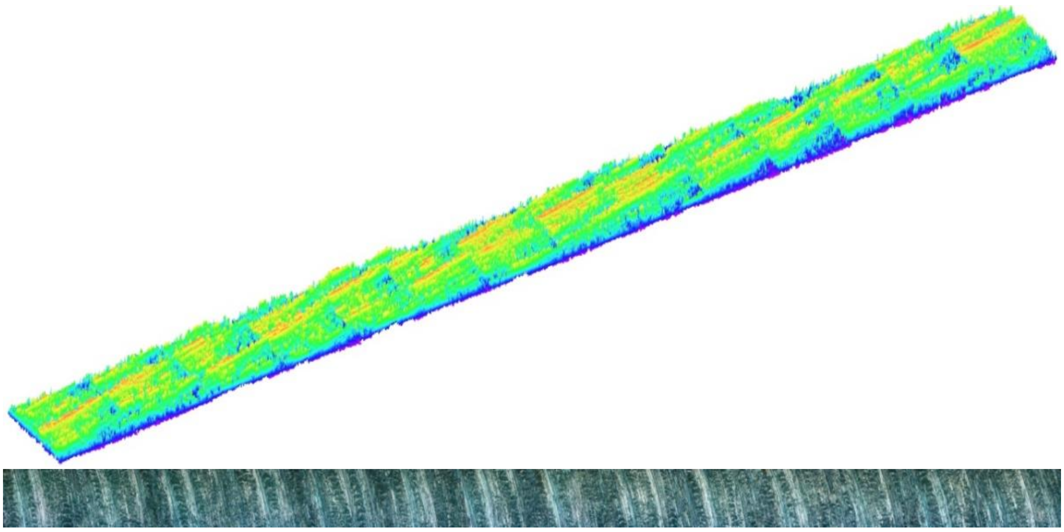

Figure 14 – The 2D and 3D images of the surfaces machined with the high-speed milling cutter (the fifth mode).

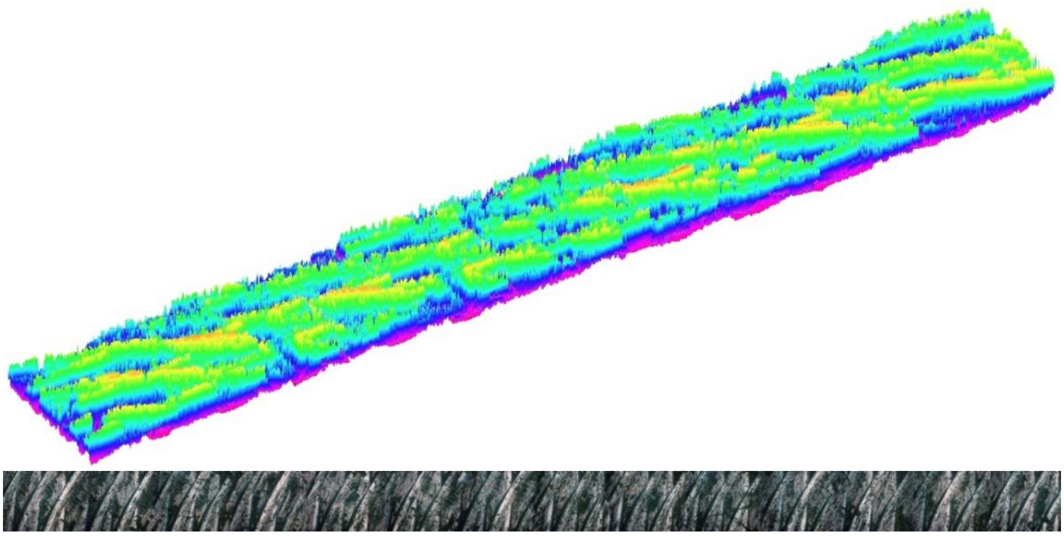

Figure 15 – The 2D and 3D images of the surfaces machined with the carbide milling cutter (the fifth mode).

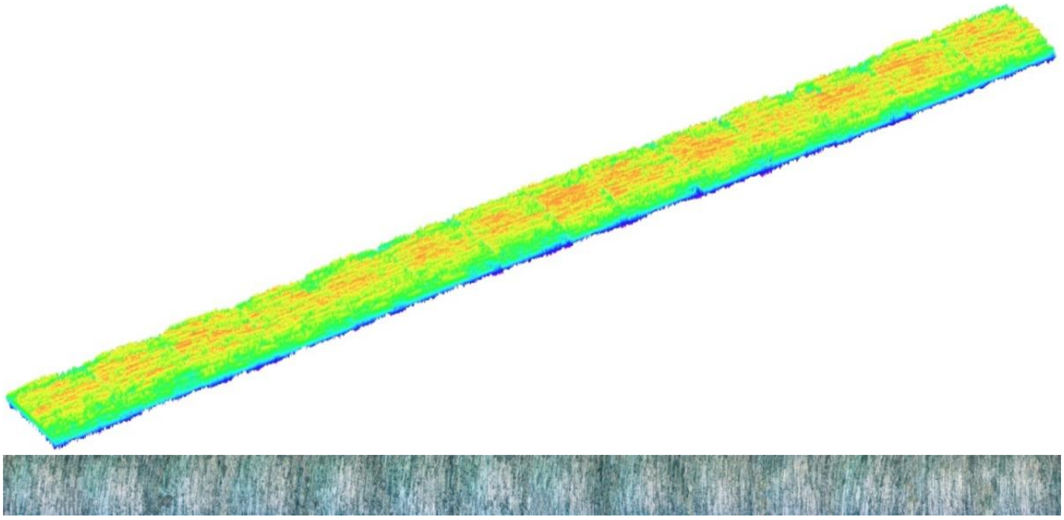

Figure 16 – The 2D and 3D images of the surfaces machined with the high-speed milling cutter (the sixth mode).

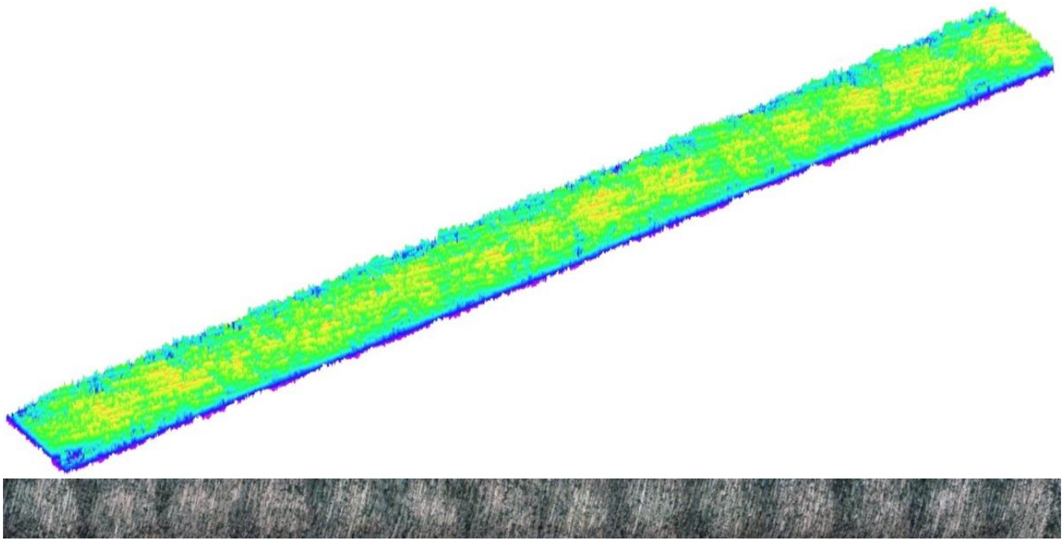

Figure 17 – The 2D and 3D images of the surfaces machined with the carbide milling cutter (the sixth mode).

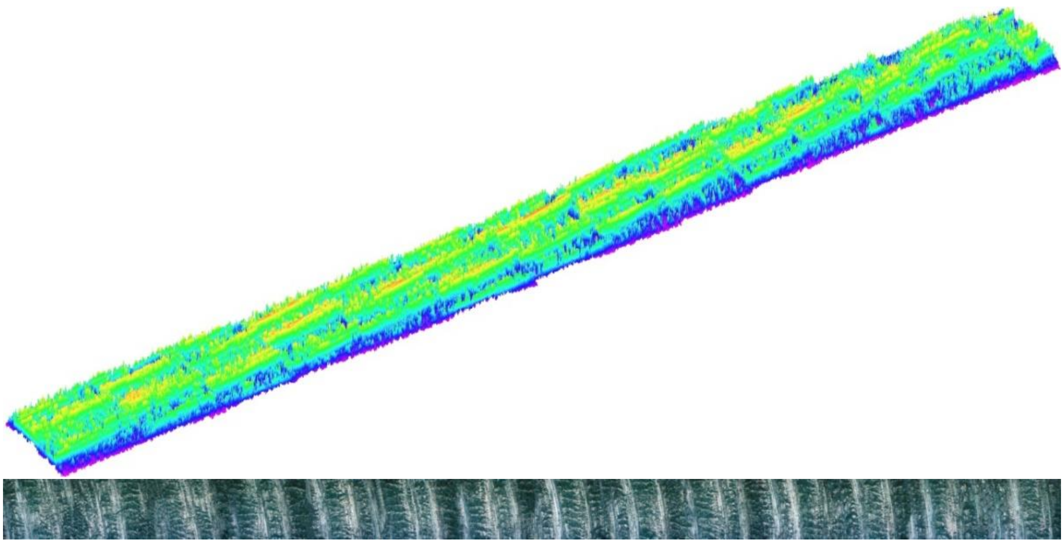

Figure 18 – The 2D and 3D images of the surfaces machined with the high-speed milling cutter (the seventh mode).

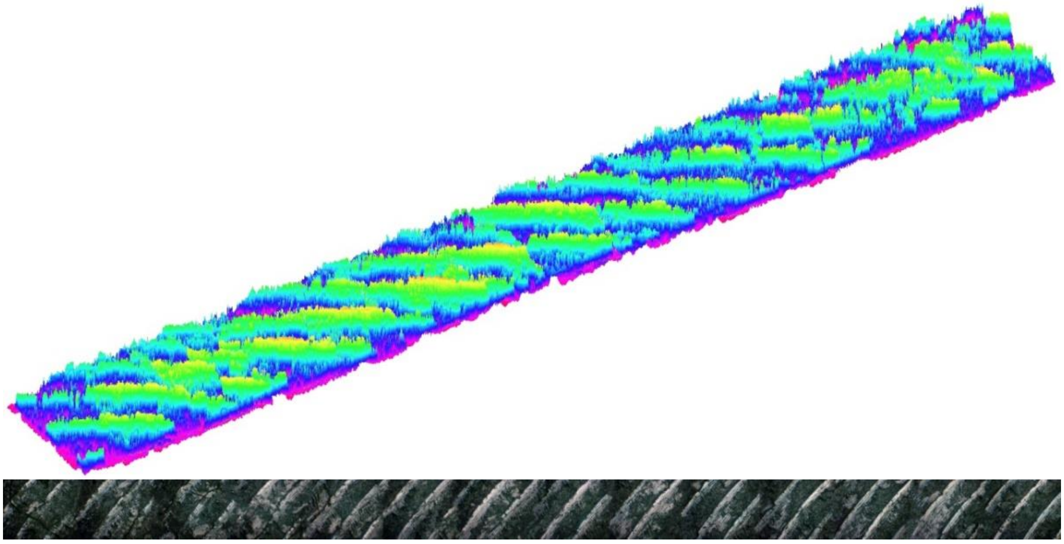

Figure 19 – The 2D and 3D images of the surfaces machined with the carbide milling cutter (the seventh mode).

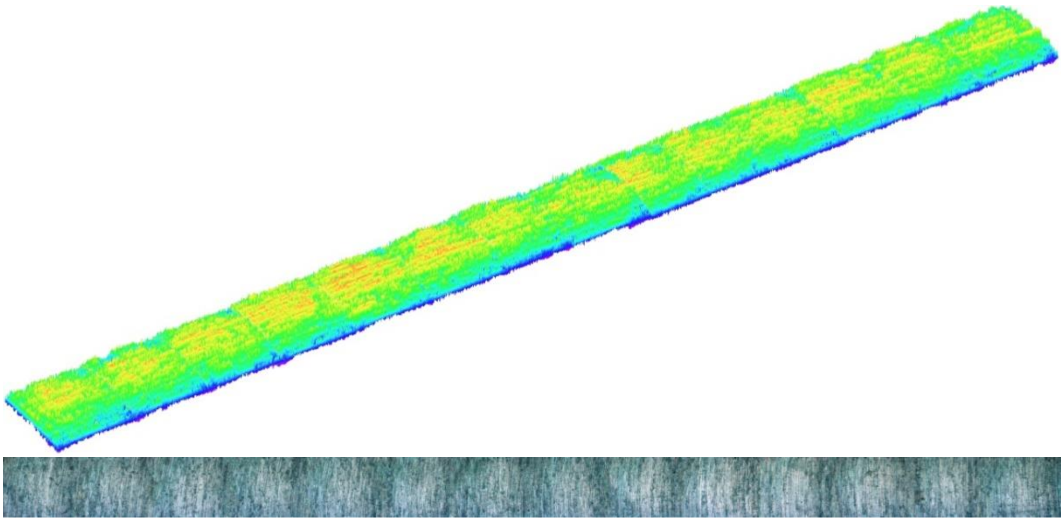

Figure 20 – The 2D and 3D images of the surfaces machined with the high-speed milling cutter (the eighth mode).

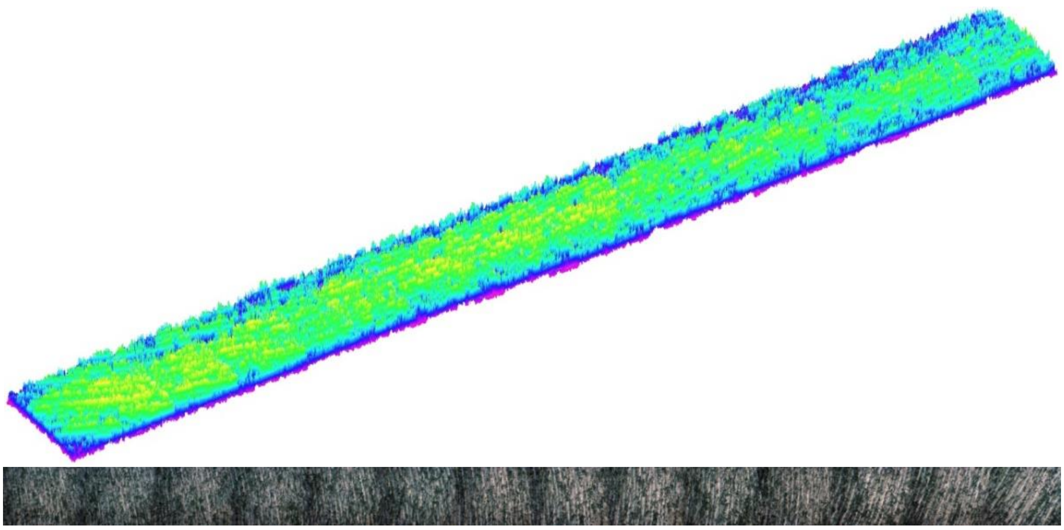

Figure 21 – The 2D and 3D images of the surfaces machined with the carbide milling cutter (the eighth mode).

Conclusion

The formation of required roughness and waviness of the machined surface is associated with a rational choice of the cutting tool material and the milling modes. For increasing the performance of machining with the formation of the desired profile of the flat surface, it is preferable to choose the high-speed milling cutter and the high speeds of semi-finishing milling. Similar low roughness of the machined surface can be obtained by reducing the feed rate of the billet. These recommendations are correct in the conditions of short-term finishing and semi-finishing milling of aluminum alloy.

References:

1. (n.d.). *GOST 2789-73. Surface roughness. Parameters and characteristics*.
2. Benardos, P. (2003). Predicting surface roughness in machining: a review. *International Journal of Machine Tools and Manufacture*, vol. 43, no. 8, 833-844.
3. Lou, M. S., Chen, J. C., & Li, C. M. (1999). Surface Roughness Prediction Technique for CNC End-Milling. *Journal of Industrial Technology*, vol. 15, no. 1, 1-6.
4. Chemezov, D., Petrenko, A., Komissarov, A., & Gorbatenko, O. (2019). Optimization of cutting modes when semifinish and rough milling. *ISJ Theoretical & Applied Science*, 08 (76), 209-213.
5. Dujun, T. A., Pchelkin, V. M., & Saharov, D. V. (2016). Study of resistance and surface roughness at milling alloy steel. *Bulletin of modern technologies*, 4(4), 47-51.
6. Beshevli, O. B., & Duyun, T. A. (2016). Empirical models surface roughness at milling babbitt. *The Bulletin of BSTU named after V. G. Shukhov*, №7, 122-127.
7. Al-Zubaidi, S., et al. (2013). Prediction of Surface Roughness When End Milling Ti6Al4V Alloy Using Adaptive Neurofuzzy Inference System. *Modelling and Simulation in Engineering*, 1-12.
8. Benardos, P. G., & Vosniakos, G. C. (2002). Prediction of surface roughness in CNC face milling using neural networks and Taguchi's design of experiments. *Robotics and Computer Integrated Manufacturing*, vol. 18, no. 5-6, 343-354.
9. Ruslan, M. S., Othman, K., Ghani, J. A., Kassim, M. S., & Haron, C. H. C. (2016). Surface roughness of magnesium alloy AZ91D in high speed milling. *J. Teknol*., 78, 115-119.
10. Makarichev, Yu. A., & Ivannikov, Yu. N. (2016). *Methods of experiment planning and data processing.* Samara State Technical University, 131 p.